The Binding Mechanism of Pyoverdin with the Outer Membrane Receptor FpvA in *Pseudomonas aeruginosa* Is Dependent on Its Iron-Loaded Status†

Emilie Clément,‡ Philippe J. Mesini,§ Franc Pattus,‡ and Isabelle J. Schalk*,‡

Departement des Récepteurs et Protéines Membranaires, UPR 9050 CNRS, ESBS, Bld Sébastien Brandt, BP 10412, F-67413 Illkirch, Strasbourg, France, and Institut Charles Sadron, 6 rue Boussingault, 67 000 Strasbourg, France

Received February 2, 2004; Revised Manuscript Received April 21, 2004

ABSTRACT: In iron-deficient conditions, *Pseudomonas aeruginosa* secretes a major fluorescent siderophore named pyoverdin (Pvd), which after chelating iron(III) is transported back into the cell via its outer membrane receptor FpvA. FpvA is a TonB-dependent transport protein and has the ability to bind Pvd in its apo- or iron-loaded form. The fluorescence properties of Pvd were used to determine the binding kinetics of metal-free and metal-loaded Pvd to FpvA and showed two major features. First, the kinetics of formation of the FpvA-Pvd complex, in vivo and in vitro, are markedly slower compared to those observed for FpvA−Pvd-metal. Second, apo-Pvd and Pvd-metal absorbed with biphasic kinetics to FpvA: the bimolecular step (association of the ligand with the receptor) is followed by a slower step ($t_{1/2}$ values of 5 and 34 min for Pvd-metal and Pvd, respectively) that presumably leads to a more stable complex. The most likely explanation for this second step is that the binding of the ligand to the receptor induces a conformational change on FpvA, which may be different, depending on the loading status of Pvd. Analysis of the dissociation of metal-free Pvd from FpvA revealed an energy and a TonB dependency. The dissociation of iron-free Pvd from FpvA in the absence of the TonB protein occurs with slow kinetics in the range of hours, but it can be highly activated by the protonmotive force and TonB to reach a kinetic with a $t_{1/2}$ of 1 min. Apparently, under iron-limited conditions, TonB activates the FpvA receptor, resulting in a fast release of iron-free Pvd and generating an unloaded FpvA receptor, competent for binding extracellular Pvd-Fe.

When grown under iron-limited conditions, many bacteria synthesize and release in the extracellular medium, iron chelators termed siderophores (*1*, *2*). These siderophores (MW usually between 300 and 2000 Da) make iron available for use by the cells by solubilizing the ferric ion of insoluble complexes that is formed under aerobic conditions (*3*−*6*).

For uptake of the ferric siderophores, Gram-negative bacteria use in the outer membrane siderophore-specific, high-affinity, active receptors. The X-ray crystal structures of three TonB-dependent iron siderophore transporters in *Escherichia coli*, FepA, FhuA, and FecA, respectively, ferric enterobactin, ferrichrome, and ferric citrate outer membrane receptors, have been solved (*7*−*11*). All structures show a similar 22-stranded β-barrel, enclosing an N-terminal plug domain. The ligand-binding surfaces on the extracellular side of these proteins are formed by residues of both the plug and the β-barrel domains. The transport into the periplasm via the specific outer membrane receptor requires the protonmotive force (pmf)[1] across the cytoplasmic membrane and an energy transduction complex that includes the cytoplasmic membrane proteins TonB, ExbB, and ExbD (*12*−*15*). The mechanism by which TonB is coupled to the pmf and how this energy is transduced to the outer membrane receptor have been mostly studied in *E. coli* and are still unknown. However, the pmf and the ligand-bound receptor drive conformational changes in TonB, suggesting a dynamic model of energy transduction in which TonB cycles through a set of conformations that differ in potential energy (reviewed in ref *16*).

Pseudomonas aeruginosa is an opportunistic human pathogen that infects injured, immunodeficient, or otherwise compromised patients. Under iron-limited conditions, *P. aeruginosa* secretes a major siderophore called pyoverdin (Pvd). Pvd is a partly cyclic octapeptide linked to a chromophore, derived from 2,3-diamino-6,7-dihydroxyquinoline, which confers color and fluorescence to the molecule (*17*, *18*). Like other TonB-dependent uptake systems, the process of iron uptake by *P. aeruginosa* begins with the binding of ferric Pvd to its specific outer membrane receptor, FpvA (*19*). The FpvA protein belongs to a subfamily of siderophore outer membrane receptors, for which a role as a regulator of transcription induction has been shown (*20*). The receptors of this family present also different structural features compared to the other siderophore outer membrane receptors.

† This work was partly funded by the Centre National de la Recherche Scientific (Programme Dynamique et Réactivité des Assemblages Biologiques) and the Association Vaincre la Mucoviscidose.

* To whom correspondence should be addressed. E-mail: schalk@esbs.u-strasbg.fr. Phone: (+33) (0) 3 90 24 47 19. Fax: (+33) (0) 3 90 24 48 29.

‡ UPR 9050 CNRS, ESBS.

§ Institut Charles Sadron.

[1] Abbreviations: Pvd, iron-free pyoverdin; Pvd-Fe, ferric pyoverdin; Pvd-Ga, pyoverdin gallium; FRET, fluorescence resonance energy transfer; pmf, protonmotive force; FCCP, carbonyl cyanide *p*-(trifluoromethoxy)phenylhydrazone; CCCP, carbonyl cyanide *m*-chlorophenylhydrazone.

10.1021/bi049768c CCC: $27.50
Published on Web 05/28/2004

They all contain an additional 70-residue extension preceding the N-terminal plug domain. Removal of this region abolishes transcription induction without affecting transport (*21*), suggesting that both siderophore transport and induction of genes are independent processes. Moreover, FecA and FpvA, two receptors of this subfamily, are able to bind their iron-free siderophore and, in the case of FpvA, with almost the same affinity as for the ferric siderophore form (10-fold difference; *19*). It has been demonstrated, for each of these two receptors, that the normal states of FecA and FepA, under iron-limited conditions, seem to be the receptor−apo-siderophore complex (*11*, *19*). Formation of the FpvA−Pvd-Fe complex, which is the first step in the iron-uptake process, occurs by the displacement of the bound Pvd with the extracellular Pvd-Fe on the FpvA receptor (*19*). The kinetics of this siderophore displacement is stimulated by TonB (*19*). For the FecA−diCit-Fe complex, ligand binding is accompanied by conformational changes in three domains of FecA: two extracellular loops (L7 and L8), one plug domain loop, and the periplasmic TonB-box motif. The large rearrangement of loops L7 and L8 in the FecA−diCit-Fe complex closes the binding site and renders diferric dicitrate inaccessible to the extracellular medium (*11*). In the FecA−diCit complex, no change of conformation has been observed in the extracellular loops of the receptor, and the FecA-bound citrate is still accessible from the extracellular medium (*11*). Similarly, time-resolved fluorescence spectroscopy studies using the spectral properties of Pvd and Pvd-Ga have shown a different proteic environment of Pvd in the in vitro formed FpvA−Pvd and FpvA−Pvd-Ga complexes: for the FpvA−Pvd-Ga complex, the Pvd is less solvent accessible and less mobile than in the FpvA−Pvd complex formed under the same experimental conditions (*22*). As the diferric dicitrate in its binding site on FecA, the Pvd-Ga seems to be trapped deeper inside the FpvA receptor compared to metal-free Pvd.

In this study, we report the binding kinetics of metal-free Pvd and metal-loaded Pvd to the FpvA receptor in vitro and in vivo using the fluorescent properties of Pvd (*23*). The binding of apo-Pvd and Pvd-metal to FpvA showed complex and different kinetics, with a mechanism depending on the metal-loaded status of the siderophore. Moreover, the fluorescent properties of Pvd have been used as well to investigate the dissociation kinetics of the FpvA−Pvd and FpvA−Pvd-metal complexes and the possible regulation by the TonB protein of these kinetics. We show for the first time that the TonB in *P. aeruginosa* is able to highly activate the release of Pvd from its receptor FpvA. Furthermore, the iron uptake via the Pvd pathway in *P. aeruginosa* will be discussed in the light of all these new and important data.

MATERIALS AND METHODS

Chemicals. Carbenicillin disodium salt was a generous gift from SmithKline Beecham (Welwyn Garden City, Herts, U.K.). The protonophores FCCP [carbonyl cyanide *p*-(trifluoromethoxy)phenylhydrazone] and CCCP (carbonyl cyanide *m*-chlorophenylhydrazone) were purchased from Sigma. Pvd, [^{3}H]Pvd, [^{3}H]Pvd-Fe, and Pvd-Ga have been prepared as described previously (*19*, *22*, *24*, *25*).

Bacterial Strains and Growth Media. The *P. aeruginosa* strains used and their phenotypes are listed in Table 1. Strain K691 is an FpvA-deficient mutant whose construction has been described previously (*23*). The Pvd-deficient strain CDC5 was originally described by Ankenbauer et al. (*26*). The mutation has been mapped to the *pvd* locus, which contains genes involved in the synthesis of the peptide moiety of pyoverdin. PAD14 is a $TonB_1$ mutant and Pvd-deficient strain, which has been described (*27*). Overproduction of FpvA in PAD14, K691, and CDC5 strains was achieved by introduction of the plasmid pPVR2 carrying the cloned *fpvA* gene (*28*).

Table 1: *P. aeruginosa* Strains Used in This Study

strain	phenotype	ref
K691(pPVR2)	$fpvA^+$ Pvd $tonB_1$ $tonB_2$	*23*
CDC5(pPVR2)	$fpvA^+$ ΔPvd $tonB_1$ $tonB_2$	*28*
PAD14(pPVR2)	$fpvA^+$ ΔPvd Δ$tonB_1$ $tonB_2$	this study

All cells were grown overnight in a iron-limited growth medium and succinate as carbon source (*25*) at 29 °C in the presence of 150 μg/mL carbenicillin for CDC5(pPVR2) and K691(pPVR2) and 50 μg/mL tetracyclin and 500 μg/mL streptomycin for PAD14(pPVR2). For all of the experiments, cells were grown overnight to an OD_{600} of 0.3−0.5. Subsequently, cells were collected by centrifugation, and the pellet was washed twice with an equal volume of fresh medium. The pellet was resuspended in 50 mM Tris-HCl (pH 8.0) to the desired OD_{600}.

Preparation of Outer Membranes and Purified FpvA Receptor. Outer membranes and purified FpvA receptor from Pvd-deficient strain CDC5(pPVR2) were prepared as described previously (*23*).

Effect of FCCP and CCCP on Iron Uptake. CDC5-(pPVR2) and PAD14(pPVR2) cells were prepared at an OD_{600} of 0.6 in 50 mM Tris-HCl (pH 8.0) buffer and incubated at room temperature in the presence of increasing concentrations of CCCP or FCCP (0−500 μM) during 15 min. Pvd-^{55}Fe was then added at a final concentration of 0.1 μM, and the mixture was incubated during 30 min. Pvd-^{55}Fe was prepared as described previously (*19*). The iron uptake was stopped by filtration of the samples on GF/B (Whatman) filters presoaked in 1% poly(ethylenimine) to reduce nonspecific retention of Pvd-^{55}Fe.

Effect of FCCP and CCCP on Cell Viability. CDC5-(pPVR2) and PAD14(pPVR2) cells were prepared at an OD_{600} of 0.05 in 50 mM Tris-HCl (pH 8.0). The bacteria were incubated in the presence or in the absence of 200 μM FCCP or CCCP at 29 °C during 15 min. After incubation, the cells were pelleted and washed twice with 2 volumes of Tris-HCl buffer containing 1 mM BSA (bovine serum albumin), followed with 2 volumes of Tris buffer, and finally, the cells were resuspended in LB medium and spread on plates.

Ligand-Binding Assays. For the in vivo and in vitro determination of the apparent dissociation constants for [^{3}H]Pvd and [^{3}H]Pvd-Fe binding to FpvA, we used the filtration assay as described previously (*19*). Since the expression level of FpvA is 3 times higher in CDC5(pPVR2) compared to PAD14(pPVR2), the CDC5(pPVR2) and PAD14(pPVR2) cells were prepared respectively at an OD_{600} of 0.05 and 0.15, in order to have the same concentration of FpvA receptors in each cell suspension. To prevent ligand depletion, leading to erroneous interpretation of ligand association data when the Scatchard plot is used (*29*), the two cell suspensions were

further diluted 5-fold in 50 mM Tris-HCl (pH 8.0) buffer. Then, the cells were incubated at 29 °C in a final volume of 500 μL in the presence of varying concentrations of [^{3}H]-Pvd (0.1−90 nM; 2.1 Ci/mmol) and [^{3}H]Pvd-Fe (0.1−80 nM; 2.1 Ci/mmol) for 2 and 1 h, respectively. All incubations were carried out at 29 °C except for CDC5(pPVR2), which was incubated in the presence of [^{3}H]Pvd-Fe. In this case, the samples were incubated at 0 °C in order to avoid iron uptake. Incubations were stopped as described previously by filtering the assay mixture (*19*). To evaluate the nonspecific binding of [^{3}H]Pvd and [^{3}H]Pvd-Fe, the binding experiment were repeated, in parallel, for each concentration of siderophore with the same strains grown in LB medium. In an iron-rich medium, no FpvA receptor is expressed.

Fluorescence Spectroscopy. FRET experiments were performed with a SPEX Fluorolog-2 or a PTI (Photon Technology International TimeMaster, Bioritech) spectrofluorometer. For all of the experiments the sample was stirred at 29 °C in a 1 mL cuvette, the excitation wavelength was set at 290 nm, and the emission of fluorescence was measured at 447 nm.

For the kinetic studies on purified FpvA, the receptor was prepared at a concentration of about 0.05 μg/mL in 1% octyl-POE and 50 mM Tris-HCl buffer (pH 8.0). Pvd-Ga and Pvd were added at different concentrations (2−50 nM for Pvd-Ga and 10−175 nM for Pvd). The emission of fluorescence at 447 nm was measured every 0.1 s for Pvd-Ga (during 900 s) and every 1 s for Pvd (during 3 h). To check the stability of the receptor at 290 nm, the experiment was repeated in the absence of siderophore. The stabilities of Pvd and Pvd-Ga at 290 nm were monitored as well. The same experiments were repeated with outer membranes prepared from Pvd-deficient FpvA-overexpressing strain CDC5 (pPVR2).

For the binding kinetics in vivo, CDC5(pPVR2) and PAD14(pPVR2) were prepared in 50 mM Tris-HCl (pH 8.0) at an OD_{600} of 0.005 and 0.015, respectively. The binding kinetics in the presence of different concentrations of Pvd-Ga and Pvd were carried out as described above for purified FpvA. For the kinetics in the presence of protonophore, the cells were prepared in Tris-HCl buffer containing 100 μM FCCP and incubated for 15 min before addition of siderophore. Measurement of the kinetics was then carried out, as described above, in the presence of 100 μM FCCP. For the binding of siderophore to FpvA, the FRET signal/noise ratio is better with purified FpvA receptor than with cells. This is not due to a different measurement statistic since we used the same counting and sampling times. This comes only from a bigger noise. The reason is that the living cell suspensions we used were not homogeneous; we clearly have a suspension with aggregates.

For the siderophore dissociation experiments, purified FpvA, at a concentration of about 0.05 μg/mL in 1% octyl-POE and 50 mM Tris-HCl buffer (pH 8.0), was incubated in the presence of 40 nM Pvd-Ga or 150 nM Pvd. When equilibrium was reached, 500 nM Pvd-Fe or 0.1 mM Pvd-Ga was added, and the decrease of fluorescence at 447 nm was monitored. For the in vivo experiments, the assay was repeated with CDC5(pPVR2) and PAD14(pPVR2) cells at an OD_{600} of respectively 0.05 and 0.1, preincubated with or without 100 μM FCCP. The Pvd-producing K691(pPVR2) cells were prepared as well at an OD_{600} of 0.05 in 50 mM Tris-HCl (pH 8.0) and 100 μM FCCP buffer. Pvd-Fe (0.1 mM) was added, and the decrease of fluorescence was monitored at 447 nm.

F/F_0 is defined as the ratio of the net fluorescence (F) by the net fluorescence intensity at the beginning of an experiment (F_0).

Data Analysis. The curves were fitted by a least-squares method. The uniqueness of the fits was checked by repeated calculations performed with distinct experimental data points (from several experiments). Additionally, several sets of initial values of parameters have been used to avoid local minima in the minimization process. Some variations among different cell batches were noted specially for the kinetics with iron-free Pvd, but within modest limits.

In most of the cases, the curves could be fitted only with a biexponential rise:

$$F(t) = F(0) + a[1 - \exp(-k_{app1}t)] + b[1 - \exp(-k_{app2}t)]$$

with

$$a + b = F(\infty) - F(0)$$

where $F(0)$ and $F(\infty)$ are the initial and final fluorescence, L is the concentration of ligand, and a and b are the amplitudes of the increase of fluorescence. For large values of L ($L \gg K_{d1}$, $K_{d1} = k_{off1}/k_{on1}$) we used the approximation

$$k_{app1} \approx k_{on1}L + k_{off1}$$

$$k_{app2} \approx k_{on2} + k_{off2}$$

For some other experiments, the curves could be fitted only with a monoexponential rise:

$$F(t) = F(0) + a[1 - \exp(-k_{app}t)]$$

with

$$a = F(\infty) - F(0)$$

and

$$k_{app} = k_{on}L + k_{off}$$

Dissociation curves were analyzed with either one or two exponentials according to the following:

$$F(t) = F(\infty) + a\exp(-k_{off}t)$$

or

$$F(t) = F(\infty) + a\exp(-k_{off1}t) + b\exp(-k_{off2}t)$$

with

$$F(0) - F(\infty) = a + b$$

a and b are given as amplitudes of the decrease (*30*).

RESULTS

Affinity of [^{3}H]Pvd and [^{3}H]Pvd-Fe for FpvA in Vivo in the Absence and in the Presence of TonB and pmf. In previous papers, we have shown that, under iron-limited

Table 2: Apparent Dissociation Constants (K_{dapp}) of [^{3}H]Pvd and [^{3}H]Pvd-Fe to FpvA Determined in Vivo[a]

strain	K_{dapp} (nM)	
	[^{3}H]Pvd (nM)	[^{3}H]Pvd-Fe (nM)
CDC5(pPVR2) (at 0 °C) (+TonB$_1$, +pmf)	6.8 ± 1.1	0.5 ± 0.1
CDC5(pPVR2) + FCCP[b] (+TonB$_1$, −pmf)	3.2 ± 0.9	0.6 ± 0.1
PAD14(pPVR2) (−TonB$_1$, +pmf)	3.2 ± 0.8	0.5 ± 0.1
PAD14(pPVR2) + FCCP[b] (−TonB$_1$, −pmf)	3.4 ± 0.4	0.7 ± 0.1

[a] The constants have been determined from a Scatchard representation, and the errors have been determined from multiple Scatchard plots. [b] FCCP was used at a concentration of 100 μM, and the cells have been preincubated during 15 min in the presence of FCCP (100 μM) befor the start of the experiment.

conditions, the normal state of FpvA in the outer membrane of *P. aeruginosa* is the FpvA−Pvd complex (*19*). During iron uptake this FpvA-bound Pvd is displaced by the extracellular Pvd-Fe, giving rise to an FpvA−Pvd-Fe complex (*19*). This siderophore exchange mechanism on FpvA is stimulated by TonB (*19*). To clarify the mechanism by which TonB activates the formation of the FpvA−Pvd-Fe complex, we compared the affinities of [^{3}H]Pvd and [^{3}H]-Pvd-Fe to FpvA in vivo, in the absence and in the presence of TonB and/or pmf, using again the filtration assay and the Scatchard analysis of the data (*19*, *23*). The experimental conditions are summarized in Table 2. For the determination of the affinities of the two forms of Pvd for FpvA in the presence of TonB and pmf, the CDC5(pPVR2) cells were placed at 0 °C (Table 1). At this temperature, the outer membrane receptors are able to bind ferric siderophores, but no uptake occurs (*29*). For the experiments in the absence of TonB, the TonB$_1$-deficient PAD14(pPVR2) (Table 1) mutant was used. In *P. aeruginosa*, two *tonB* genes have been identified, *tonB*$_1$ and *tonB*$_2$ (*31*). *TonB*$_1$ is directly involved in ferric pyoverdin uptake, since disruption of only the *tonB*$_1$ gene abrogates siderophore-mediated iron uptake (*31*). Deletion of the *tonB*$_2$ gene does not adversely affect growth on iron-restricted medium. For the experiments performed in the absence of pmf, the concentration of protonophore used has been determined from the assay described in Figure 1. In this experiment, CDC5(pPVR2) cells were incubated in the presence of Pvd-^{55}Fe and of increasing concentrations of FCCP or CCCP, and the ^{55}Fe uptake was followed in time. The same inhibitor effect on the iron uptake has been observed for both FCCP and CCCP, namely, a total inhibition at 100−150 μM protonophore. The viability of *P. aeruginosa* cells at this concentration of FCCP is about 80% (*32*). In all of the binding experiments carried out in vivo, the nonspecific binding was estimated by repeating the same experiment with cells grown in LB medium. Since the expression of the FpvA receptor is regulated by the iron concentration in the extracellular medium, FpvA will not be expressed when cells are grown in this medium. The nonspecific binding has been subtracted for the determination of the K_d.

Table 2 summarizes the apparent K_d determined for [^{3}H]-Pvd-Fe and [^{3}H]Pvd in the different studied conditions. In all cases, the same amount of FpvA receptors was able to bind [^{3}H]Pvd and [^{3}H]Pvd-Fe with about a 10-fold difference

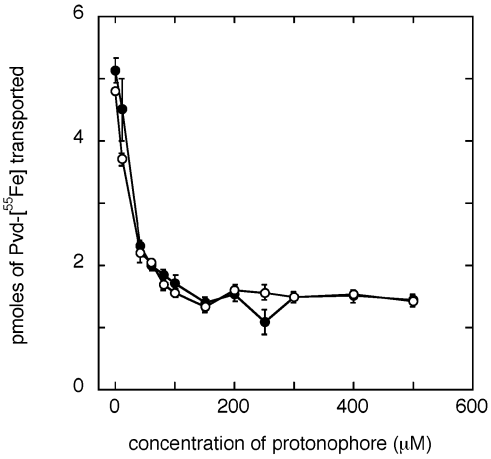

FIGURE 1: Effect of CCCP and FCCP on Pvd-^{55}Fe uptake. CDC5-(pPVR2) cells at an OD_{600} of 0.6 were preincubated during 15 min in the presence of increasing concentrations of CCCP (●) or FCCP (○) (0−500 μM). Subsequently, 0.1 μM Pvd-^{55}Fe was added, and the cells were incubated for another 30 min. The iron uptake was stopped by filtration as described in Materials and Methods.

in their affinities. Moreover, the affinity of [^{3}H]Pvd and [^{3}H]-Pvd-Fe for FpvA seems to be TonB$_1$ and pmf independent.

PaA-Ga Binds Faster to FpvA than Metal-Free Pvd. According to the data presented in Table 2, pmf and TonB do not regulate the affinity of FpvA for Pvd and Pvd-Fe. But a similar K_d does not involve necessarily the same association (k_{on}) and dissociation (k_{off}) kinetic constants ($K_d = k_{off}/k_{on}$). These kinetic constants may vary in a way to keep a constant K_d. To test this possibility, the fluorescent properties of Pvd were used to study the binding kinetics of Pvd and Pvd-metal to FpvA. Because of the presence of a 2,3-diamino-6,7-dihydroxyquinoline chromophore, Pvd is a really interesting fluorescent siderophore having the spectral properties to interact by FRET with the Trps of FpvA (maximum of absorption at 380 nm and emission of fluorescence at 447 nm; *23*). Only iron-free Pvd is fluorescent. After complexation with iron(III), the metal quenches the fluorescence of Pvd, and FRET cannot be observed for the FpvA−Pvd-Fe complex. A fluorescent Pvd-metal complex can be obtained by complexing Pvd with Ga. We have shown previously that the Pvd-Ga complex has the same affinity for FpvA and is transported with the same velocity as the ferric form (*22*). To study the FpvA receptor, our group has already used the Pvd-Ga complex to visualize different mechanistic aspects of the interaction between FpvA and its siderophore, using time-resolved fluorescence spectroscopy (*22*).

The data presented in Figure 2 show the difference in the binding kinetics between Pvd and Pvd-Ga for FpvA. The TonB$_1$- and Pvd-deficient PAD14(pPVR2) (OD_{600} = 0.6) strain has been incubated in the presence of 200 nM Pvd-Ga or Pvd, and the fluorescence was monitored at 447 nm (excitation wavelength set at 290 nm). In the absence of TonB, the siderophore outer membrane receptor is able to bind its unloaded or metal-loaded siderophore, but no transport occurs. The increase of fluorescence observed in Figure 2 represents the formation of the FpvA-Pvd (○) or FpvA−Pvd-Ga complex (△). As illustrated in Figure 2, the binding of Pvd and Pvd-Ga to the FpvA receptor is different in terms of amplitude and time course. First, the equilibrium

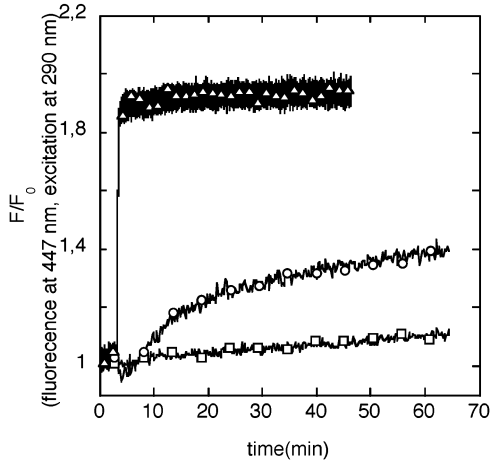

FIGURE 2: Binding of Pvd and Pvd-Ga monitored by FRET in the $TonB_1$-deficient PAD14(pPVR2) cells. $TonB_1$-deficient and FpvA-overproducing PAD14(pPVR2) cells were resuspended in 50 mM Tris-HCl (pH 8.0) at an OD_{600} of 0.6, and the emission of fluorescence at 447 nm was monitored at 29 °C. After 120 s, Pvd (○) and Pvd-Ga (△) were added at a final concentration of 200 nM, and the emission of fluorescence at 447 nm was monitored during 1 h. The experiment was repeated without addition of siderophore (□). The kinetics in the absence of siderophore has been subtracted from the kinetics in the presence of siderophore before calculation of F/F_0.

is reached within a few minutes in the presence of Pvd-Ga, and only after 1 h in the presence of metal-free Pvd, showing clearly that metal-free Pvd binds slower to the FpvA receptor in vivo than metal-loaded Pvd. The difference in the ratio F/F_0 is due to a difference in the occupancy of the siderophore binding sites on FpvA (Pvd-Fe has a 7-fold better affinity for FpvA than apo-Pvd; Table 2).

Pvd-Ga Binding to FpvA: Determination of the Binding Kinetic Constants in Vitro. To determine accurately the kinetic constants (k_{on} and k_{off}) of the binding of Pvd-Ga to purified FpvA, different concentrations (from 2 to 50 nM) of Pvd-Ga were added to the purified FpvA receptor. We chose ligand concentrations [L] at least 1 order of magnitude higher than the total receptor concentration [R_T] ([L] > 10[R_T]) to reach pseudo-first-order conditions. The samples were excited at 290 nm (excitation wavelength of the Trp), and the emission of fluorescence was measured at 447 nm (emission of fluorescence of Pvd-Ga) as a function of time. Figure 3A shows the time course for purified FpvA incubated in the presence of 7.5 and 15 nM Pvd-Ga. As in Figure 2, the increase of the Pvd-emitted fluorescence at 447 nm reflects the occupancy of receptors by the fluorescent ligand. The experimental binding trace for each studied concentration of Pvd-Ga was fitted by a sum of two exponentials revealing a two-step binding with two apparent association rate constants (k_{app1} and k_{app2}). The first step is a rapid process in the second time range, representing 90% of the FRET amplitude. In agreement with a bimolecular reaction scheme, its apparent rate increases linearly with ligand concentration (Figure 2B), with a slope equal to 9.6×10^5 M^{-1} s^{-1} representing k_{on1} (Table 3). The intercept with the ordinate axis gives an estimation of the dissociation rate constant for this first rapid step ($k_{off1} = 0.0056$ s^{-1}; Table 3). The second step develops in the minute time range, and its apparent rate constant is roughly constant with respect to the concentration of Pvd-Ga (Figure 2B and Table 3). Since $k_{app2} \approx k_{on2} +$

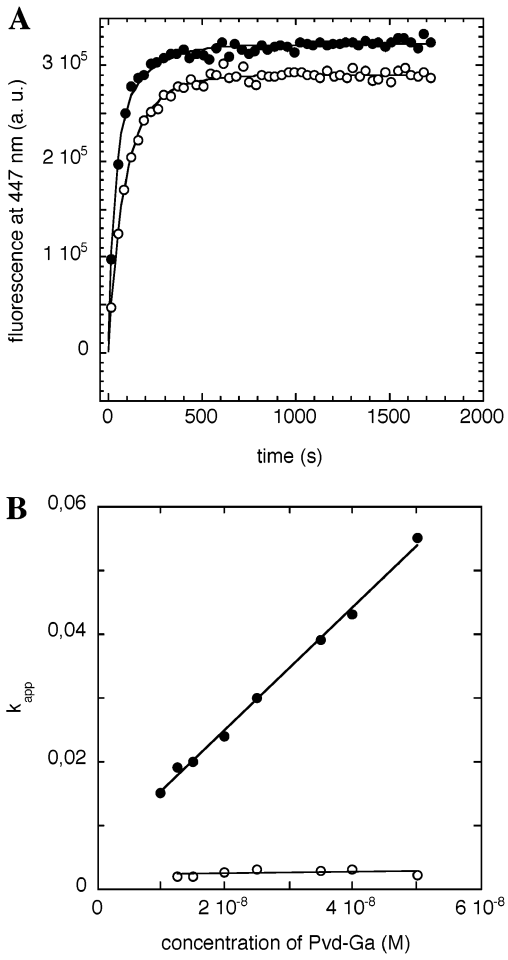

FIGURE 3: Time recording of Pvd-Ga binding to purified FpvA. (A) Time course of Pvd-Ga binding to purified FpvA. Purified FpvA in 50 mM Tris-HCl (pH 8.0) and 1% octyl-POE was incubated in the presence of 7.5 nM (○) and 15 nM (●) Pvd-Ga, and the emission of fluorescence was monitored at 447 nm (excitation at 290 nm). Data were fitted to the theoretical time course for a two-component exponential model (solid line). (B) Plot of apparent rate constants k_{1app} (●) and k_{2app} (○) versus Pvd-Ga concentration. k_{1app} and k_{2app} were determined from fitting binding traces of the binding of Pvd-Ga to purified FpvA receptor with two exponentials. The solid lines through the data points were obtained by fitting with eq 1 under Materials and Methods.

k_{off2}, if k_{off2} can be neglected in respect to k_{on2}, one has $k_{app2} \approx k_{on2}$ ($k_{on2} = 0.0024$ s^{-1}). This plateau is in agreement with the equation more classically used, $k_{app2} = k_{on2}[L/(L + K_{d1})] + k_{off2}$ (*33*), and corresponds to the case where $L \gg K_{d1}$. Because of the limitation of the technique of FRET used, k_{app2} could not be determined for low concentrations of Pvd-Ga. Indeed, the second step of binding represents a low increase of FRET amplitude (about 10% of the total amplitude) and could be hardly estimated at low concentration of Pvd-Ga. A simply kinetic scheme, involving the binding of Pvd-Ga to the FpvA receptor, followed by a rate-limiting isomerization toward a more stable state (Scheme 1), may fit the data.

The same experiment was repeated with outer membranes of CDC5(pPVR2) cells. The number of receptors present in these membranes was estimated from radiolabeled [^{3}H]Pvd-Fe binding. The kinetic constants (k_{on1}, k_{off1}, and k_{on2}) determined are of the same order of magnitude as for the purified FpvA receptor and are summarized in Table 3.

Scheme 1: Kinetic Model for the Binding of Pvd-Metal and Apo-Pvd to FpvA[a]

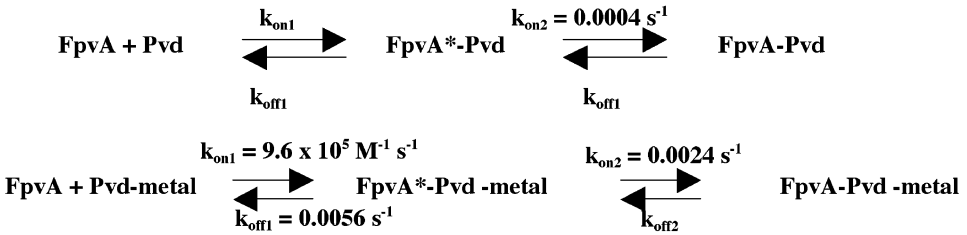

[a] The equilibria represent a minimal kinetic binding model derived from in vivo and in vitro binding data.

Table 3: Pvd-Ga Binding Rate Constants for the FpvA Receptor[a]

	rate constant	value	$t_{1/2}$[c]
purified FpvA[b]	k_{on1}	$9.6 \times 10^5\ M^{-1}\ s^{-1}$	1 min 12 s
			7 s
	k_{off1}	$0.0056\ s^{-1}$	2 min
	k_{on2}	$0.0024\ s^{-1}$	5 min
outer membrane[b]	k_{on1}	$2.7 \times 10^6\ M^{-1}\ s^{-1}$	26 s
			3 s
	k_{off1}	$0.0078\ s^{-1}$	1 min 20
	k_{on2}	$0.0053\ s^{-1}$	2 min
CDC5(pPVR2) + FCCP[d] (+TonB$_1$, −pmf)	k_{on1}	$1.7 \times 10^6\ M^{-1}\ s^{-1}$	41 s
			4 s
	k_{off1}	$0.0075\ s^{-1}$	1 min 30
	k_{on2}	$0.0034\ s^{-1}$	3 min 20
PAD14(pPVR2) (−TonB$_1$, +pmf)	k_{on1}	$2.8 \times 10^6\ M^{-1}\ s^{-1}$	25 s
			3 s
	k_{off1}	$0.0027\ s^{-1}$	4 min 30
	k_{on2}	$0.001\ s^{-1}$	11 min 30
PAD14(pPVR2) + FCCP[d] (−TonB$_1$, −pmf)	k_{on1}	$2.7 \times 10^6\ M^{-1}\ s^{-1}$	26 s
			3 s
	k_{off1}	$0.0040\ s^{-1}$	3 min
	k_{on2}	$0.0041\ s^{-1}$	3 min

[a] Rate constants determined from in vitro and in vivo fluorescence binding time courses are summarized for the interconversions in Scheme 1. Constants were determined at 29 °C in 50 mM Tris-HCl (pH 8.0) and for the purified FpvA receptor in the presence of 1% octyl-POE. [b] Purified FpvA and outer membranes were prepared from Pvd-deficient strain CDC5(pPVR2) cells. [c] The $t_{1/2}$ values were calculated from the respective constants using the relationship $t_{1/2} = 0.693/k$. For k_{on1}, $t_{1/2}$ was calculated for a concentration of Pvd-Ga of first 10 nM and then 100 nM to compare with the Pvd data in Table 4. [d] FCCP was used at a concentration of 100 μM, and the cells were preincubated during 15 min in the presence of FCCP (100 μM) before the start of the experiment.

Pvd-Ga Binding to FpvA: Determination of the Binding Kinetic Constants in Vivo. Three different in vivo conditions have been studied where Pvd-Ga binds to the FpvA receptor but no transport occurs. First, the binding of Pvd-Ga to the FpvA receptor was studied in vivo in the absence of TonB and in the presence of pmf. For this purpose, TonB$_1$-deficient PAD14(pPVR2) cells (Table 1) were used. The same experiment was repeated in TonB$_1$-producing CDC5(pPVR2) cells pretreated with the protonophore FCCP at a concentration of 100 μM. Under these two conditions, the FpvA receptor is able to bind Pvd-Ga, but no uptake occurs because of the absence of pmf or TonB$_1$. For the FRET experiments, the protonophore FCCP was used instead of CCCP, because of its lower absorbance at 400 nm (a 2.5-fold difference). Finally, as a control experiment, PAD14(pPVR2) cells pretreated with the protonophore FCCP were used. As for the experiments in vitro, different concentrations (from 2 to 50 nM) of Pvd-Ga were added to the cells under pseudo-first-order conditions ([L] > 10[R$_T$]; [R$_T$] is the total receptor concentration). The mixtures were excited at 290 nm, and the emission of fluorescence was measured at 447 nm in function of time. Figure 4A shows the time course of the binding of 15 nM Pvd-Ga to FpvA in CDC5(pPVR2) cells treated with FCCP. The different time courses have been analyzed like the in vitro data with a double exponential. The kinetic rates determined from the plot of the apparent rate constants versus the Pvd-Ga concentration (Figure 4B) are summarized in Table 3. These data clearly show that in

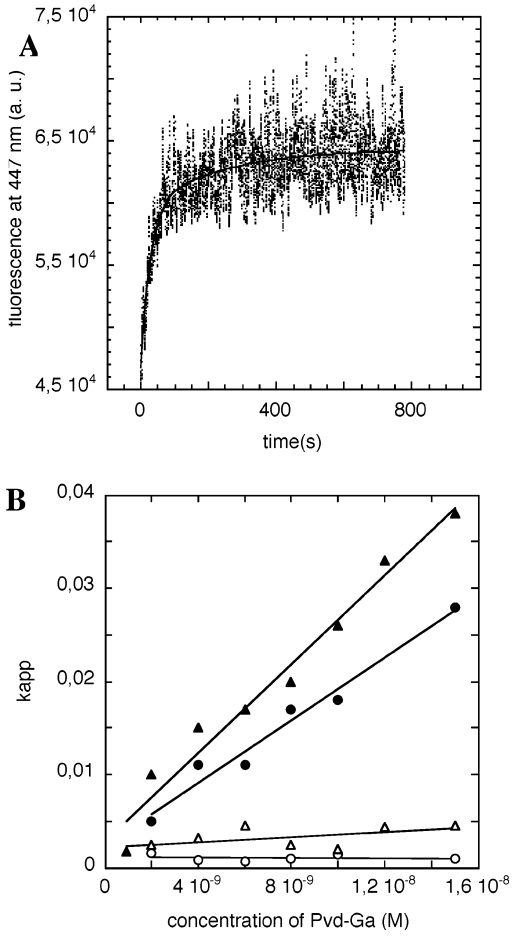

FIGURE 4: Time recording of Pvd-Ga binding to FpvA in vivo. (A) Time course of Pvd-Ga binding to FpvA in CDC5(pPVR2) cells preincubated in the presence of 100 μM FCCP. Cells were diluted in 50 mM Tris-HCl (pH 8.0) supplemented with 100 μM FCCP, at an OD_{600} of 0.005, and incubated in the presence of 15 nM Pvd-Ga; subsequently the emission of fluorescence was monitored at 447 nm (excitation at 290 nm). Data were fitted to the theoretical time course for a double exponential model (solid line). (B) Plot of apparent rate constants k_{1app} and k_{2app} versus Pvd-Ga concentration. k_{1app} (●, ▲) and k_{2app} (○, △) for the binding of Pvd-Ga to FpvA in CDC5(pPVR2) and PAD14(pPVR2) cells, respectively, were determined from fitting binding traces with the double exponential. The solid lines through the data points were obtained by fitting with eq 1 under Materials and Methods.

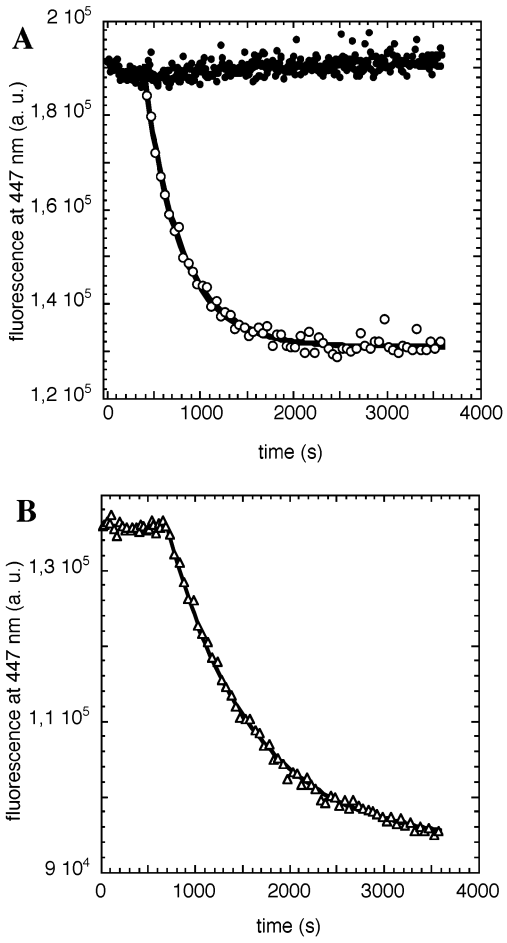

FIGURE 5: In vitro and in vivo Pvd-Ga dissociation time course. (A) For the in vitro, purified FpvA receptor (○) was preincubated for at least 30 min with 40 nM Pvd-Ga. Afterward, the dissociation of Pvd-Ga is initiated by rapid mixing with buffer containing 500 nM Pvd-Fe. The solid lines are the best fits obtained with a single exponential. For purified FpvA the experiment has been repeated in the absence of addition of Pvd-Fe (●). (B) For the in vivo dissociation, the experiment was repeated by mixing CDC5(pPVR2) cells (△), preincubated for at least 30 min with 40 nM Pvd-Ga, with buffer containing 500 nM Pvd-Fe. To avoid Pvd-Fe or Pvd-Ga uptake, the CDC5(pPVR2) cells have been pretreated with 100 μM FCCP. The solid lines are the best fits obtained with a single exponential.

vivo, in the absence of pmf and TonB, Pvd-Ga binds to the FpvA receptor as in vitro, with a biphasic kinetic and with binding kinetic constants of the same order of magnitude (Scheme 1).

Dissociation of Pvd-Ga Bound to FpvA. Dissociation of receptor−ligand complexes, obtained at equilibrium with 40 nM Pvd-Ga, was initiated by rapid mixing with a large excess (500 nM) of Pvd-Fe. The experiment was first carried out with purified FpvA receptor (Figure 5A) and then in vivo with CDC5(pPVR2) cells pretreated with the protonophore FCCP (100 μM) (Figure 5B). The dissociation of the FpvA−Pvd-Ga complex and the formation of the FpvA−Pvd-Fe complex was followed in time by monitoring the loss of fluorescence energy transfer. Ferric Pvd is not fluorescent, because iron(III) completely quenches the chromophore fluorescence (*23*). Both dissociation relaxations were best represented using a single exponential process (in vitro, $k_{app} = 0.0025\ s^{-1}$, $t_{1/2} = 5$ min; in vivo, $k_{app} = 0.0011\ s^{-1}$, $t_{1/2} = 10$ min). The determined k_{app} probably represents the limiting values of the kinetic rate constants k_{off1} and k_{off2} presented in Scheme 1 for the release of Pvd-Ga in the dissociation process. The 2-fold difference between the in vitro and in vivo kinetic rates is probably not significant and may be due to a difference in the receptor concentration and/or to the higher signal/noise ratio in vivo.

Metal-Free Pvd Binding to FpvA: Determination of the Binding Kinetic Constants in Vitro and in Vivo. The kinetic constants of the binding of iron-free Pvd to FpvA were determined using again the technique of FRET (excitation at 290 nm and emission of fluorescence recorded at 447 nm). As was shown in Figure 2, the binding of Pvd to FpvA is slower compared to Pvd-Ga; therefore, the emission of fluorescence was monitored during 3 h with integration times of 1 s instead of 0.1 s. Different concentrations (from 10 to 150 nM) of iron-free Pvd were added to the purified FpvA receptor under pseudo-first-order conditions ($[L] > 10[R_T]$; $[R_T]$ is the total receptor concentration). Figure 6A shows the time course for purified FpvA incubated in the presence of 20, 30, 40, and 60 nM Pvd. Again, the increase of the Pvd emitted fluorescence at 447 nm reflects the occupancy of receptors by the fluorescent ligand. A single exponential best described binding of iron-free Pvd to purified FpvA. In a bimolecular reaction the association kinetic rate increases linearly with the concentration of ligand. The apparent kinetic rate (k_{app}) determined for this binding is independent of the concentration of Pvd, which shows that the limiting step is not bimolecular. Most likely, Pvd binds in a two-step process like Pvd-Ga, with two apparent association rate constants (k_{app1} and k_{app2}; Scheme 1), but only the second step, which must be noticeably slower than the first one, is visualized by the used technique of FRET and occurs with a k_{app2}, independent of the concentration of Pvd, of $0.0004\ s^{-1}$ ($t_{1/2} = 30$ min). The first step cannot be seen either because this step is too fast and only accessible via stopped-flow kinetics or because Pvd is not close enough to a Trp to allow FRET. In the second step a change of conformation of FpvA or a different binding of Pvd to FpvA produces a FRET signal. When performing an excitation at 290 nm and monitoring the emission of fluorescence at 447 nm, only the kinetics of this second step is followed.

The kinetic constants for the binding of iron-free Pvd to FpvA in vivo could not be determined. Indeed, it is not possible to have the same batch of bacteria in the same physiological state in order to repeat 3 h kinetic experiments in the presence of different concentrations of Pvd. For this reason, the binding of Pvd to FpvA was studied in vivo (in the presence and in the absence of $TonB_1$ and/or pmf) only for a concentration of 100 nM Pvd. In vivo (Figure 6B), as in vitro, the time course of the binding is best described by a single exponential. As shown in Table 4, the apparent kinetic rate determined for the binding of iron-free Pvd to FpvA is neither TonB nor pmf modulated.

Dissociation of Metal-Free Pvd Bound to FpvA. Dissociation of receptor−ligand complexes obtained with 150 nM Pvd was initiated by rapid mixing with a large excess (1 μM) of Pvd-Fe. In the different experiments presented in Figure 7, the binding of iron-free Pvd to FpvA is monitored by the increase of fluorescence at 447 nm. Afterward, the dissociation of the FpvA−Pvd complex and the formation of the FpvA−Pvd-Fe complex with time was followed by monitoring the decrease of fluorescence energy transfer. The

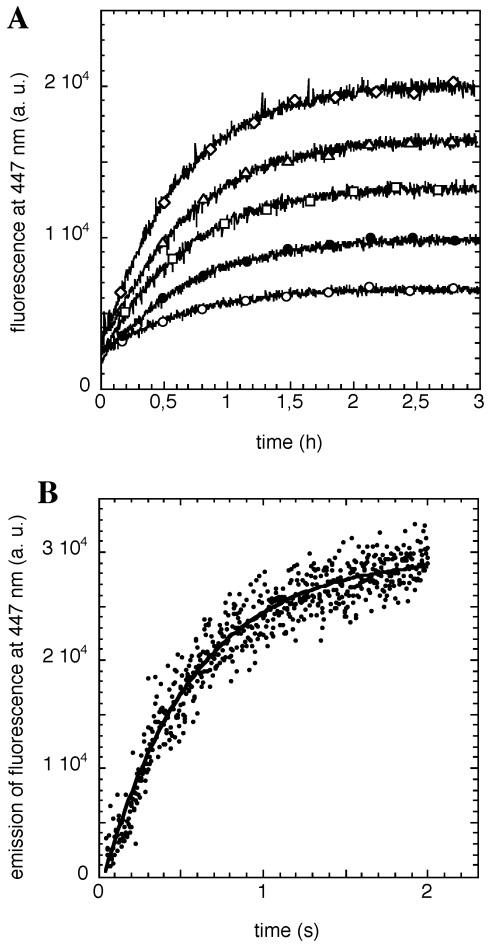

FIGURE 6: Time recording of metal-free Pvd binding to FpvA in vitro and in vivo. (A) Time course of Pvd binding to purified FpvA. Purified FpvA in 50 mM Tris-HCl (pH 8.0) and 1% octyl-POE was incubated in the presence of 10 nM (○), 20 nM (●), 30 nM (□), 40 nM (△), and 60 nM (◇) Pvd, and the emission of fluorescence was monitored at 447 nm (excitation at 290 nm). The experiment has been repeated without addition of siderophore and subtracted from the kinetics in the presence of siderophore. Data were then fitted to the theoretical time course by a single exponential (solid line). (B) Time course of Pvd binding to FpvA in CDC5-(pPVR2) cells. Cells diluted in 50 mM Tris-HCl (pH 8.0) at an OD_{600} of 0.005 were incubated in the presence of 15 nM Pvd, and the emission of fluorescence was monitored at 447 nm (excitation at 290 nm) (●). As above, the experiment has been repeated without addition of siderophore and subtracted from the kinetics in the presence of siderophore. Data were then fitted to the theoretical time course by a single exponential (solid line).

experiment was carried out in vitro with purified FpvA (Figure 7A) and in vivo in the absence (Figure 7B) and in the presence of $TonB_1$ (Figure 7C,D).

For the experiment with purified FpvA receptor (Figure 7A), identical dissociation relaxations were obtained for different preincubation times (association step): 20, 60, and 180 min. The dissociation traces obtained are best described by a single-exponential relaxation ($k_{app} = 0.0001$ s^{-1}, $t_{1/2} =$ 2 h; Table 4). The determined k_{app} probably represents the limiting values of the kinetic rate constants k_{off1} and k_{off2} presented in Scheme 1 for the release of apo-Pvd in the dissociation process.

The experiment was repeated in vivo with the $TonB_1$-deficient PAD14(pPVR2) cells preincubated in the presence of 150 nM Pvd for 80 min (Figure 7B). In the absence of

Table 4: Iron-Free Pvd Binding Rates Constants for the FpvA Receptor[a]

	rate constant	value (s^{-1})	$t_{1/2}$[c] (min)
purified FpvA[b]	k_{app1}	0.00034	34
outer membrane[b]	k_{app1}	0.00024	48
CDC5(pPVR2) + FCCP[d]	k_{app1}	0.00045	26
CDC5(pPVR2)	k_{app1}	0.0005	23

[a] The apparent association kinetic rates were determined from in vitro and in vivo fluorescence time courses at 29 °C in 50 mM Tris-HCl (pH 8.0) in the presence of 100 nM Pvd. For the purified FpvA receptor, the experiment was carried out in the presence of 1% octyl-POE. [b] Purified FpvA and outer membranes were prepared from Pvd-deficient strain CDC5(pPVR2) cells. [c] The $t_{1/2}$ values were calculated from the respective constants using the relationship $t_{1/2} = 0.693/k$. [d] FCCP was used at a concentration of 100 μM, and the cells were preincubated during 15 min in the presence of FCCP (100 μM) before the start of the experiment.

$TonB_1$ the FpvA receptor is able to bind the ferric siderophore, but no transport occurs (*31*). According to the kinetics presented in Figure 7B, in the absence of $TonB_1$, Pvd hardly dissociates from FpvA. However, the added Pvd-Fe competes with Pvd for the remaining empty FpvA binding site at the cell surface and decreases the binding kinetic rate of iron-free Pvd.

The Pvd dissociation experiment was repeated in vivo in the presence of energy and the TonB machinery with CDC5-(pPVR2) cells and is summarized in Figure 7C. Under these experimental conditions, the dissociation of Pvd from FpvA, which is shown by the decrease of fluorescence at 447 nm, is fast with a $t_{1/2} = 4$ min (30-fold faster than in vitro). Once the equilibrium is reached, the fluorescence increases slightly due to the recycling of Pvd (after iron release) on the FpvA receptor (*34*). When the experiment is repeated in the presence of the protonophore FCCP, the dissociation of Pvd from FpvA is slowed down as in Figure 7B, confirming that the $TonB_1$ protein regulates the dissociation of iron-free Pvd. The experiment presented in Figure 7C demonstrates also that only a few FpvA receptors are activated by $TonB_1$ and involved in the iron uptake.

As documented previously (*22*), two procedures can be used to prepare the FpvA−Pvd complex. Either the complex is prepared in vitro as described above or it is preformed in vivo from a *P. aeruginosa* Pvd- and FpvA-producing strain and subsequently purified. Time-resolved fluorescent spectroscopy has shown that the FpvA−Pvd complex undergoes two different conformations depending on how it was prepared (*22*). When the FpvA−Pvd complex has been formed in vivo, the polarity of the environment of Pvd, its solvent accessibility, and its rotational dynamics are much slower than for the in vitro formed complex. Previous in vitro experiments on the purified in vivo formed FpvA−Pvd complex have shown a dissociation half-life time of 25 h (*19*). In Figure 7D, the experiment was repeated in vivo by incubation of K691(pPVR2) cells in the presence of an excess of Pvd-Fe (1 μM). Strain K691(pPVR2) produces Pvd, which explains the increase of fluorescence before addition of Pvd-Fe ($t = 120$ s). After addition of an excess of Pvd-Fe, the dissociation of iron-free Pvd with the in vivo formed FpvA−Pvd complex is fast in the presence of the $TonB_1$ protein ($t_{1/2} = 1$ min; Figure 7D) and is shown by the decrease of fluorescence at 447 nm. Afterward, the increase of fluorescence after 250 s shows the recycling of

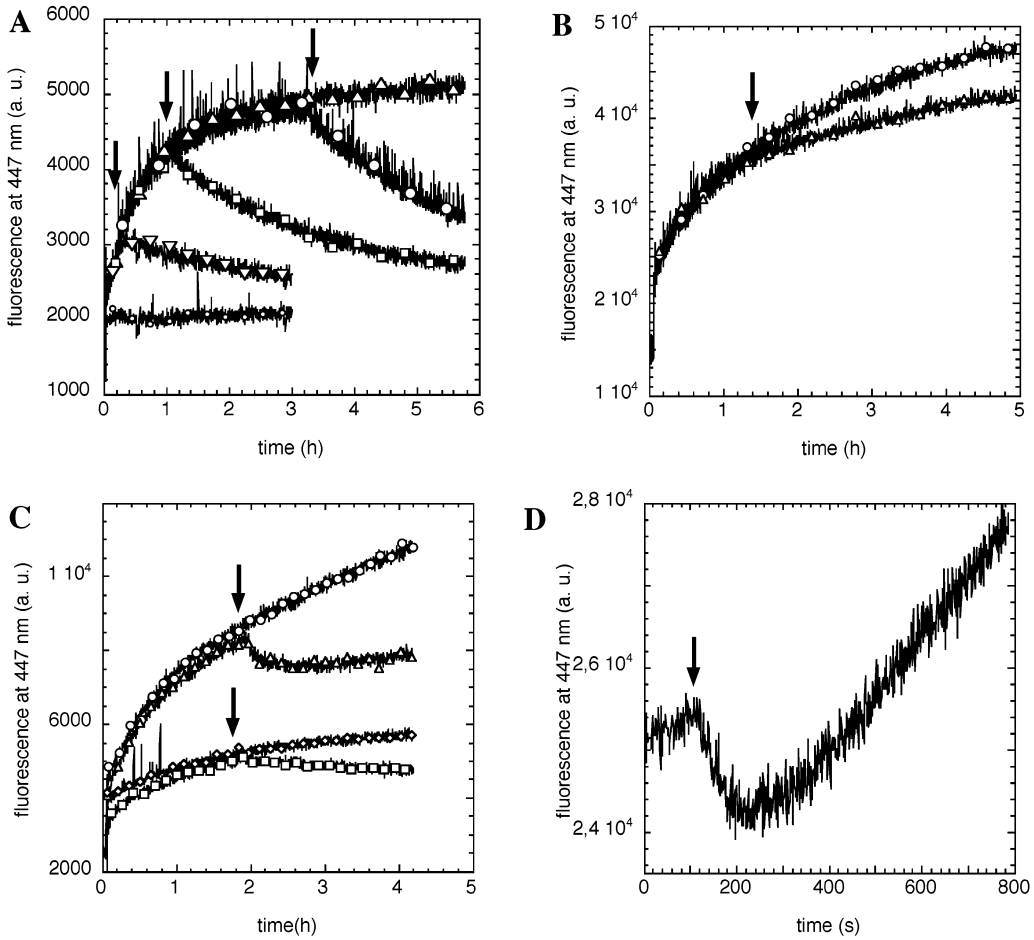

FIGURE 7: In vitro and in vivo iron-free Pvd dissociation time courses. (A) Dissociation of Pvd in vitro (purified FpvA). In vitro dissociation of Pvd is initiated by rapid mixing of purified FpvA receptor preincubated for 20 min (▽), 60 min (□), and 180 min (○) with 150 nM Pvd before addition of buffer containing 1 μM Pvd-Fe. The experiment was repeated without addition of Pvd-Fe (△) and without addition of Pvd and Pvd-Fe (□). (B) Dissociation in vivo in a $TonB_1$-deficient strain. Dissociation of Pvd is initiated by rapid mixing of the $TonB_1$-deficient PAD14(pPVR2) cells preincubated for 80 min with 150 nM Pvd before addition of buffer containing 1 μM Pvd-Fe (△). The experiment was repeated without addition of Pvd-Fe (○). (C) Dissociation of Pvd in vivo in the presence or in the absence of pmf. Dissociation of Pvd is initiated by rapid mixing of the Pvd-deficient CDC5(pPVR2) cells preincubated for 80 min with 150 nM Pvd before addition of buffer containing 1 μM Pvd-Fe (△). The experiment was repeated without addition of Pvd-Fe (○). Both experiments with (□) or without (◇) addition of Pvd-Fe have been repeated in the presence of 100 μM FCCP. (D) Dissociation in vivo in a Pvd-producing *P. aeruginosa* strain. Dissociation of Pvd is initiated by rapid mixing of the Pvd- and FpvA-producing K691(pPVR2) cells with buffer containing 1 μM Pvd-Fe. In these strains the FpvA−Pvd complex is formed in vivo. In all experiments the addition of Pvd-Fe is shown by an arrow.

Pvd on FpvA and the continuous secretion of the synthesized Pvd by the cells. This recycling step has been described previously (*34*).

DISCUSSION

FpvA and the *E. coli* FecA receptors have particular features compared to other siderophore outer membrane receptors. In addition to the ability to transport ferric siderophore, they are able to bind their corresponding iron-free siderophore (*11*, *19*, *23*, *34*, *35*) and to regulate the transcription of genes involved in the iron uptake (*36*, *37*). In this study we have investigated the property of FpvA to bind iron-free and iron-loaded Pvd (*19*) and its implication in the Pvd pathway iron-uptake mechanism. The fluorescent properties of Pvd have shown that under iron-limited conditions all of the FpvA receptors at the cell surface are loaded with iron-free Pvd (*19*). Binding assays using tritiated Pvd and Pvd-Fe demonstrated that both forms of Pvd bind with close affinities, and with a stoichiometry of 1, to a common or overlapping binding site on FpvA (*19*, *22*). In parallel, the X-ray structures of FecA−diCit and FecA−diCit-Fe have shown that iron-free and iron-loaded dicitrate bind as well to a common binding site on FecA (*11*, *38*). However, the relative orientations of the two citrate ions are different in the two structures. For the hemophore receptor in *Serratia marcescen*, Létoffé et al. have shown that apo- and holo-hemophore are able to bind with the same affinity to the same binding site on HasR (*38*).

Binding of Pvd-Ga and Pvd to FpvA. The data presented in this paper point out clearly a different mechanism for the binding of apo-Pvd and metal-loaded Pvd to FpvA. The displacement experiment (Figures 5 and 7) shows that Pvd and Pvd-metal are in competition for a common or overlapping binding site on FpvA. The binding affinities (K_d) of both forms of Pvd are close, with a 10-fold difference in favor of Pvd-metal (Table 1 and refs *19* and *23*). However, the kinetics presented in Figure 2 show that the formation of the FpvA−Pvd-metal complex is faster compared to the formation of FpvA-Pvd. A more precise analysis of these kinetics showed a two-step binding for Pvd and Pvd-Ga

(Scheme 1).

For Pvd-Ga, the first step is fast, in the range of seconds (Table 3), and corresponds probably to the binding of the ligand to the receptor. The second step, which is slower, in the range of minutes (Table 3), may correspond to the formation of a more stable FpvA−Pvd-Ga complex (Scheme 1). Considering that Pvd-Ga and Pvd-Fe have the same affinities for the FpvA receptor and are transported with the same velocity (*22*), the binding mechanism shown for Pvd-Ga can probably be extended to Pvd-Fe. Such biphasic association kinetics have been reported also for the binding of ferric enterobactin or ColB to FepA in *E. coli*, with a fast binding component and a secondary slower component (*39*).

Similarly to metal-loaded Pvd, metal-loaded Pvd binds in a two-step process to the FpvA receptor. The apparent kinetic rate (k_{app}) determined for the kinetic time courses presented in Figure 6 is independent of the concentration of Pvd, showing that the limiting step is not bimolecular. Probably, iron-free Pvd binds in a two-step process, with the first one being markedly faster than the second one. In that way the kinetics of the bimolecular stage does not affect the kinetics of the second stage. The first step cannot be seen either because this step is too fast and only accessible via stopped-flow kinetics or because Pvd is not in close proximity of a Trp and FRET cannot occur. In the second stage, Pvd may bind differently to the FpvA receptor, or the binding of Pvd induces a change of conformation in FpvA, which brings one or more Trps close to the bound Pvd. In Folschweiller et al., a Foerster distance of 13 Å has been determined between Pvd and the Trp involved in FRET in the purified FpvA−Pvd complex (*22*). If we suppose the existence of a first binding site, on one of the extracellular loops of FpvA, and a second one closer to the plug domain, the distance between them is about 20−30 Å, according to the X-ray structures of FhuA (*10*), FepA (*7*), or FecA (*8*, *11*). Moreover, the extracellular loops of FpvA are poor in Trps. Indeed, in FhuA, FecA, and FepA, most of the Trps form an aromatic girdle positioned to extend into the lipid bilayer and delineate the border between the lipid hydrocarbon chains and the polar headgroups. The stabilization step is about 10-fold slower for iron-free Pvd compared to metal-loaded Pvd, probably due to a difference in the 3D structure of Pvd and Pvd-metal and to a difference in the mechanism of interaction between FpvA and both forms of Pvd. The kinetics of this second binding step of Pvd is $TonB_1$ and energy independent (Table 4); indeed, the same apparent kinetic rate is observed in the presence or in the absence of the TonB machinery.

This biphasic binding process (Scheme 1) of Pvd and Pvd-metal strongly suggests either a mechanism with two binding sites for the siderophore (one localized on the level of the extracellular loops and the second one deeper in the protein) or a conformational change occurs in the receptor induced by the adsorption of the siderophore. Previously published time-resolved fluorescent spectroscopy studies have shown a different proteic environment for the Pvd chromophore in the FpvA−Pvd and FpvA−Pvd-Ga complexes. Indeed, the polarity of the environment of Pvd, its solvent accessibility, and its rotational dynamics are much slower in the FpvA−Pvd-Ga complex compared to FpvA−Pvd (*22*). Moreover, the 3D structure of FecA−diCit-Fe shows that the binding of ferric dicitrate induces a change in the conformation of two extracellular loops (L7 and L8), which form the lid of the siderophore-binding pocket (*11*). This large rearrangement of the L7 and L8 loops closes the lid of the binding pocket and renders the ligand inaccessible to the extracellular medium. On the contrary, the binding of iron-free citrate induces only a small change in the conformation of L7 and L8. In this complex, these loops slightly constrict the binding pocket, without closing it completely. One can imagine that the second step in the binding of Pvd and Pvd-metal to FpvA may be related, as in FecA, to a change of conformation of some extracellular loops.

Release of Pvd-Ga and Pvd from FpvA. The mutual exclusion of one ligand by the binding of the other allowed measurement of the dissociation rates of Pvd or Pvd-metal from FpvA. In contrast to the biphasic association kinetics observed for Pvd and Pvd-Ga, their dissociation rates followed single-component first-order decays (Figure 5). However, the determined k_{offapp} probably represents only the limiting values of the rate constants (k_{off1} and k_{off2}; Scheme 1) for the release of Pvd or Pvd-Ga. For Pvd-Ga, the dissociation process is in the range of minutes ($k_{off} = 0.0011$ s^{-1}, $t_{1/2} = 10$ min; Figure 5).

For metal-free Pvd, two different methods have been used to prepare the FpvA−Pvd complex. Either the complex is prepared in vitro by incubating purified FpvA in the presence of Pvd and Pvd-Ga or it is preformed in vivo from a *P. aeruginosa* Pvd- and FpvA-producing strain and subsequently purified. For the FpvA−Pvd complex, the data presented here show that this complex can exist in different conformations: (i) an in vivo formed FpvA−Pvd complex, which is extremely stable in the absence of $TonB_1$ [$t_{1/2}$ = 24 h (*23*)], (ii) an in vitro formed FpvA−Pvd complex, which according to the data presented in Figure 7A,B is less stable in the absence of $TonB_1$ (determined on purified FpvA, $t_{1/2} = 2$ h, $k_{app} = 0.0001$ s^{-1}, Figure 7A; determined in living cells, $t_{1/2} > 2$ h, Figure 7B) compared to the in vivo one, and (iii) a $TonB_1$-activated FpvA−Pvd complex which has a short half-life time ($t_{1/2} = 4$ min, Figure 7C; $t_{1/2} = 1$ min, Figure 7D). The mechanism involved in the activation of the FpvA−Pvd complex by the $TonB_1$ machinery to get release of Pvd is unknown. It probably involves some change of conformation of the FpvA receptor which decreases the stability of the FpvA−Pvd complex and the affinity of the receptor for Pvd ($K_d = k_{off}/k_{on}$). Moreover, Figure 7C clearly shows that only a few FpvA receptors are activated by the TonB protein to release Pvd. TonB is a limiting factor when many TonB-dependent uptake systems are induced (*40*) and even more in conditions of overexpression of outer membrane receptors. In addition, this activation of TonB seems to be fast and for these different reasons cannot be seen under the experimental conditions used in Table 2 to determine the K_d. To better understand the mechanism of activation of the release of Pvd from FpvA by the $TonB_1$ machinery, the $TonB_1$/ExbB/ExbD machinery should be overexpressed at the same level as the FpvA receptor. However, it is the first time that TonB is shown to be involved in the activation of an outer membrane receptor to get a fast release of the bound apo siderophore. This new biological function of TonB undeniably must play a role in the iron uptake mechanism via Pvd in *P. aeruginosa*.

Ferric Pvd Uptake Mechanism in P. aeruginosa. Clearly, different intermediate states must exist in the transport

mechanism of a ligand-gated channel like FpvA. Under iron-limited conditions, all of the receptors at the cell surface are loaded with iron-free Pvd. By a yet unknown mechanism, this FpvA−Pvd complex is dissociated with a fast kinetic rate by the action of the $TonB_1$ machinery in vivo. Since $TonB_1$ is limiting compared to the amount of FpvA receptors at the cell surface, only a few FpvA−Pvd complexes are activated to get release of Pvd. Once the FpvA receptor has its binding site free, extracellular Pvd and Pvd-Fe competes with similar affinities for this binding site. The data in Figure 2 clearly show that at equivalent concentration, metal- loaded Pvd binds much faster to the FpvA receptor than iron-free Pvd. Once the FpvA−Pvd-Fe complex is formed, the $TonB_1$ machinery activates the receptor to get transport of the ferric siderophore into the periplasm. Taken together, a multitude of questions remain to be answered. Among others, what is the mechanism for the activation of the FpvA−Pvd complex by the $TonB_1$ protein to get release of the iron-free Pvd? What is the mechanism of activation of the FpvA−Pvd-Fe complex by $TonB_1$ to get uptake of iron? Elucidation of the exact role of TonB in this activation process will be a goal for future studies.

ACKNOWLEDGMENT

We thank Dr. Hendrick Adams and Dr. Mohamed Abdallah for critically reading the manuscript.

REFERENCES

1. Neilands, J. B. (1995) Siderophores: Structure and Function of Microbial Iron Transport Compounds, *J. Biol. Chem. 270*, 26723−26726.
2. Boukhalfa, H., and Crumblis, A. L. (2002) Chemical aspects of siderophore mediated iron transport, *Biometals 15*, 325−339.
3. Andrews, S. C., Robinson, A. K., and Rodriguez-Quinones, F. (2003) Bacterial iron homeostasis, *FEMS Microbiol. Rev. 27*, 215−237.
4. Braun, V. (1998) Pumping iron through cell membranes, *Science 282*, 2202−2203.
5. Braun, V., Hantke, K., and Koster, W. (1998) Bacterial iron transport: mechanisms, genetics, and regulation, *Met. Ions Biol. Syst. 35*, 67−145.
6. Braun, V., and Braun, M. (2002) Active transport of iron and siderophore antibiotics, *Curr. Opin. Microbiol. 5*, 194−201.
7. Ferguson, A. D., Hofmann, E., Coulton, J. W., Diederichs, K., and Welte, W. (1998) Siderophore-mediated iron transport: crystal structure of FhuA with bound lipopolysaccharide, *Science 282*, 2215−2220.
8. Ferguson, A. D., Chakraborty, R., Smith, B. S., Esser, L., van der Helm, D., and Deisenhofer, J. (2002) Structural basis of gating by the outer membrane transporter FecA, *Science 295*, 1715−1719.
9. Buchanan, S. K., Smith, B. S., Venkatramani, L., Xia, D., Esser, L., Palnitkar, M., Chakraborty, R., van der Helm, D., and Deisenhofer, J. (1999) Crystal structure of the outer membrane active transporter FepA from *Escherichia coli*, *Nat. Struct. Biol. 6*, 56−63.
10. Locher, K. P., Rees, B., Koebnik, R., Mitschler, A., Moulinier, L., Rosenbusch, J. P., and Moras, D. (1998) Transmembrane signaling across the ligand-gated FhuA receptor: crystal structures of free and ferrichrome-bound states reveal allosteric changes, *Cell 95*, 771−778.
11. Yue, W. W., Grizot, S., and Buchanan, S. K. (2003) Structural evidence for iron-free citrate and ferric citrate binding to the TonB-dependent outer membrane transporter FecA, *J. Mol. Biol. 332*, 353−368.
12. Postle, K. (1993) TonB protein and energy transduction between membranes, *J. Bioenerg. Biomembr. 25*, 591−601.
13. Kadner, R. J. (1990) Vitamin B12 transport in *Escherichia coli*: energy coupling between membranes, *Mol. Microbiol. 4*, 2027−2033.
14. Bradbeer, C. (1993) The proton motive force drives the outer membrane transport of cobalamin in *Escherichia coli*, *J. Bacteriol. 175*, 3146−3150.
15. Larsen, R. A., Myers, P. S., Skare, J. T., Seachord, C. L., Darveau, R. P., and Postle, K. (1996) Identification of TonB homologues in the family Enterobacteriaceae and evidence for conservation of TonB-dependent energy transduction complexes, *J. Bacteriol. 178*, 1363−1373.
16. Postle, K., and Kadner, R. J. (2003) Touch and go: tying TonB to transport, *Mol. Microbiol. 49*, 869−882.
17. Demange, P., Bateman, A., Mertz, C., Dell, A., Piemont, Y., and Abdallah, M. A. (1990) Bacterial siderophores: structure and NMR assigment of pyoverdins PaA, siderophores of *Pseudomonas aeruginosa* ATCC 15692, *Biochemistry 29*, 11041−11051.
18. Wendenbaum, S., Demange, P., Dell, A., Meyer, J. M., and Abdallah, M. A. (1983) The structure of pyoverdin Pa, the siderophore of *Pseudomonas aeruginosa*, *Tetrahedron Lett. 24*, 4877−4880.
19. Schalk, I. J., Hennard, C., Dugave, C., Poole, K., Abdallah, M. A., and Pattus, F. (2001) Iron-free pyoverdin binds to its outer membrane receptor FpvA in *Pseudomonas aeruginosa*: a new mechanism for membrane iron transport, *Mol. Microbiol. 39*, 351−360.
20. Visca, P., Leoni, L., Wilson, M. J., Lamont, I. L., and Doring, G. (2002) Iron transport and regulation, cell signaling and genomics: lessons from *Escherichia coli* and Pseudomonas, *Mol. Microbiol. 45*, 1177−1190.
21. Kim, I., Stiefel, A., Plantor, S., Angerer, A., and Braun, V. (1997) Transcription induction of the ferric citrate transport genes via the N-terminus of the FecA outer membrane protein, the Ton system and the electrochemical potential of the cytoplasmic membrane, *Mol. Microbiol. 23*, 333−344.
22. Folschweiller, N., Gallay, J., Vincent, M., Abdallah, M. A., Pattus, F., and Schalk, I. J. (2002) The interaction between pyoverdin and its outer membrane receptor in *Pseudomonas aeruginosa* leads to different conformers: a time-resolved fluorescence study, *Biochemistry 41*, 14591−14601.
23. Schalk, I. J., Kyslik, P., Prome, D., van Dorsselaer, A., Poole, K., Abdallah, M. A., and Pattus, F. (1999) Copurification of the FpvA ferric pyoverdin receptor of *Pseudomonas aeruginosa* with its iron-free ligand: implications for siderophore-mediated iron transport, *Biochemistry 38*, 9357−9365.
24. Albrecht-Garry, A. M., Blanc, S., Rochel, N., Ocacktan, A. Z., and Abdallah, M. A. (1994) Bacterial iron transport: coordination properties of pyoverdin PaA, a peptidic siderophore of *Pseudomonas aeruginosa*, *Inorg. Chem. 33*, 6391−6402.
25. Demange, P., Wendenbaum, S., Linget, C., Mertz, C., Cung, M. T., and Dell, A., and Abdallah, M. A. (1990) Bacterial siderophores: structure and NMR assigment of pyoverdins PaA, siderophores of *Pseudomonas aeruginosa* ATCC 15692, *Biol. Met. 3*, 155−170.
26. Ankenbauer, R., Hanne, L. F., and Cox, C. D. (1986) Mapping of mutations in *Pseudomonas aeruginosa* defective in pyoverdin production, *J. Bacteriol. 167*, 7−11.
27. Takase, H., Nitanai, H., Hoshino, K., and Otani, T. (2000) Requirement of the *Pseudomonas aeruginosa* tonB gene for high-affinity iron acquisition and infection, *Infect. Immun. 68*, 4498−4504.
28. Poole, K., Neshat, S., Krebes, K., and Heinrichs, D. E. (1993) Cloning and nucleotide sequence analysis of the ferripyoverdine receptor gene fpvA of *Pseudomonas aeruginosa*, *J. Bacteriol. 175*, 4597−4604.
29. Newton, S. M., Igo, J. D., Scott, D. C., and Klebba, P. E. (1999) Effect of loop deletions on the binding and transport of ferric enterobactin by FepA, *Mol. Microbiol. 32*, 1153−1165.
30. Lecat, S., Bucher, B., Mely, Y., and Galzi, J. L. (2002) Mutations in the extracellular amino-terminal domain of the NK2 neurokinin receptor abolish cAMP signaling but preserve intracellular calcium responses, *J. Biol. Chem. 277*, 42034−42048.
31. Zhao, Q., and Poole, K. (2000) A second tonB gene in *Pseudomonas aeruginosa* is linked to the exbB and exbD genes, *FEMS Microbiol. Lett. 184*, 127−132.
32. Royt, P. W. (1990) Pyoverdine-mediated iron transport. Fate of iron and ligand in *Pseudomonas aeruginosa*, *Biol. Met. 3*, 28−33.

33. Palanche, T., Ilien, B., Zoffmann, S., Reck, M. P., Bucher, B., Edelstein, S. J., and Galzi, J. L. (2001) The neurokinin A receptor activates calcium and cAMP responses through distinct conformational states, *J. Biol. Chem. 276*, 34853−34861.
34. Schalk, I. J., Abdallah, M. A., and Pattus, F. (2002) Recycling of Pyoverdin on the FpvA Receptor after Ferric Pyoverdin Uptake and Dissociation in *Pseudomonas aeruginosa*, *Biochemistry 41*, 1663−1671.
35. Schalk, I. J., Abdallah, M. A., and Pattus, F. (2002) Recycling of Pyoverdin on the FpvA Receptor after Ferric Pyoverdin Uptake and Dissociation in *Pseudomonas aeruginosa*, *Biochem. Soc. Trans. 30*, 702−705.
36. Braun, V., and Braun, M. (2002) Iron transport and signaling in *Escherichia coli*, *FEBS Lett. 529*, 78.
37. Visca, P., Leoni, L., Wilson, M. J., and Lamont, I. L. (2002) Iron transport and regulation, cell signaling and genomics: lessons from *Escherichia coli* and *Pseudomonas*, *Mol. Microbiol. 45*, 1177−1190.
38. Letoffe, S., Deniau, C., Wolff, N., Dassa, E., Delepelaire, P., Lecroisey, A., and Wandersman, C. (2001) Haemophore-mediated bacterial haem transport: evidence for a common or overlapping site for haem-free and haem-loaded haemophore on its specific outer membrane receptor, *Mol. Microbiol. 41*, 439−450.
39. Payne, M. A., Igo, J. D., Cao, Z., Foster, S. B., Newton, S. M., and Klebba, P. E. (1997) Biphasic binding kinetics between FepA and its ligands, *J. Biol. Chem. 272*, 21950−21955.
40. Kadner, R. J., and Heller, K. J. (1995) Mutual inhibition of cobalamin and siderophore uptake systems suggests their competition for TonB function, *J. Bacteriol. 177*, 4829−4835.

BI049768C